Supplementary Figures

Supplementary Figure 1. M290 targets CD103$^+$ cells *in vivo*. (A) CD11c$^+$ MLN cells from WT and CD103$^{-/-}$ mice were incubated with M290 or GLIII/10 (green) for 30 min on ice, then fixed, permeabilized and co-stained for EEA-1 (red) and the nuclear stain DAPI (Blue). M290 bound a subset of CD11c$^+$ MLN cells only from WT but not CD103$^{-/-}$ mice (arrow). Scale bars, 10 μm. (B) C57BL/6 mice were injected i.p. with Alexa647-M290 or Alexa647-GLIII/10 (10 μg). Animals were sacrificed after 17 h and binding of M290 (blank) or GLIII/10 (filled) to CD11c$^+$, B220$^+$ and CD8$^+$ cells from the MLN, spleen, and small intestinal lamina propria (SI-LP) was assessed by flow cytometry. Results are representative FACS plots from 1 representative experiment of 3 performed. Cells from mice injected with GLIII/10 showed similar fluorescent profiles to un-injected control mice. Numbers represent the mean (SEM) of M290$^+$ cells within the CD11c$^+$ gate compared to an isotype control. (C) Splenic and MLN sections from mice receiving Alexa647-M290 were stained with anti-B220 and anti-CD11c antibody. Alexa647-M290 was readily detected on MLN but rarely on splenic CD11c$^+$ cells (arrows). Scale bar, 100 μm. The boxed region shows a higher magnification. Scale bar, 10 μm. CD11c$^-$ M290$^+$ cells (stars) likely represent CD8$^+$ T cells. Results are representative images from one mouse of three examined.

Supplementary Figure 2. M290.OVA pulsed MLN DCs induce OT-I T cell proliferation *in vitro*. (A) Antibody/OVA conjugates were resolved by SDS-PAGE followed by immunoblotting with HRP-conjugated anti-OVA to confirm the conjugation and the removal of free OVA from the antibody/OVA mixtures. (B) CD11c$^+$ MLN DCs or (C) sorted CD103$^+$ and CD103$^-$ MLN DCs were pulsed with

(B) graded doses or (C) 1 μg/ml of antibody/OVA conjugates, washed and co-cultured with OT-I cells and assessed for [^{3}H]thymidine uptake as described in Materials and Methods. To calculate proliferation index in (C), proliferation induced by GLIII/10.OVA was set to 1. Results are from 1 representative experiment of (B) 4 or (C) 2 performed with 10 mice pooled/experiment.

Supplementary Figure 3. OT-I and OT-II cells proliferate to a similar extent in the MLN of CD103$^{-/-}$ and WT mice following i.p. immunization with high dose OVA. CFSE labeled OT-I and OT-II cells were injected i.v. into WT and CD103$^{-/-}$ mice. Mice were immunized i.p. with OVA (0.5 mg) and (A) CFSE dilution in transferred cells from WT (blank) and CD103$^{-/-}$ (filled) mice and (B) the numbers of OT-I and OT-II cells in the MLN were assessed 3 d later by flow cytometry. Results are representative FACS plots (A) and mean (SEM) of 1 experiment with 3 mice/group.

Supplementary Figure 4. **M290 and low dose OVA fails to induce OT-I and OT-II proliferation *in vivo***. C57BL/6 were injected i.v. with CFSE-labeled CD45.1$^+$ OT-I and OT-II cells. Mice were immunized i.p. with M290.OVA (1 μg) and LPS (50 μg), M290 (1 μg) together with OVA (1 μg) and LPS (50 μg) or OVA (1 μg) and LPS (50 μg) and the (A) CFSE dilution and (B) number of OT-I and OT-II cells in the MLN assessed 3 d later by flow cytometry. (A) Representative FACS plots from mice receiving M290.OVA (blank) or M290 and OVA (filled) and (B) mean (SEM) from 1 experiment with 3 mice per group. *, $p < 0.05$; ***, $p < 0.001$.

Supplementary Figure 5. CD11c$^+$ cell depletion abrogates the ability of M290.OVA to induce antigen specific T cell responses. CFSE labeled CD45.1$^+$ OT-I and OT-II cells were injected i.v. into DTx treated (shaded) or untreated (blank) CD11c.DTR mice 20 h before receiving M290.OVA (1 μg) + LPS (50 μg). Mesenteric LN (MLN), spleen and mediastinal LN (med. LN) were collected 2 d later and cell division in transferred cells analyzed by flow cytometry. Representative FACS plots from one experiment of three performed with 5 mice in total.

Supplementary Figure 6. **Intratracheal administration of M290.OVA induces T cell priming in mediastinal LN and CD4$^+$ T cell mediated tolerance.** (A) CFSE labeled OT-I and OT-II cells were injected into recipient mice and proliferation assessed in mediastinal LN 3 d after i.t. administration of M290.OVA (28 ng) or GLIII/10.OVA (56 ng) or OVA alone (56 ng). Mean number of OT-I and OT-II cells in mediastinal lymph nodes from one representative experiment of 3 performed with 2-3 mice/group. (B) Mucosal application of M290.OVA induces tolerance. Seven d after i.t. administration of M290.OVA (28 ng), GLIII/10.OVA (56 ng) or OVA (100 μg) mice were immunized with OVA and alum i.p. followed by OVA-aerosol challenges. Histological sections stained with PAS reagent. Scale bars, 100 μm. Results shown are representative sections from one mouse/group of three performed.

Video 1. M290 is internalized by MLN DC and localizes within early endosomes. MLN DCs were incubated for 60 min at 37^{0}C with Alexa-488 labeled M290, Cells were then fixed, permeabilized and stained for the early endosomal marker EEA-1. M290 (green), EEA-1 (red), Nuclei (DAPI, blue). Co-localization of M290 with endosomes appears as yellow staining. The images were acquired as 0.3 μm optical

sections spanning the entire cell with Axiovert 200M fluorescent microscope. Acquisition, deconvolution, 3D reconstruction and video were prepared using Volocity software.

Video 2. M290 was occasionally observed localizing with lysosomes. MLN DCs were incubated with Alexa-488 labeled M290 for 60 min at 37^0C. Cells were then fixed, permeabilized and stained for LAMP-1. M290 (green), LAMP-1 (purple). Co-localization of M290 with LAMP-1^+ lysosomes appears as light blue. The images were acquired as 0.3 μm optical sections spanning the entire cell with Axiovert 200M fluorescent microscope. Acquisition, deconvolution, 3D reconstruction and video were prepared using Volocity software.

Supplementary Figure 1

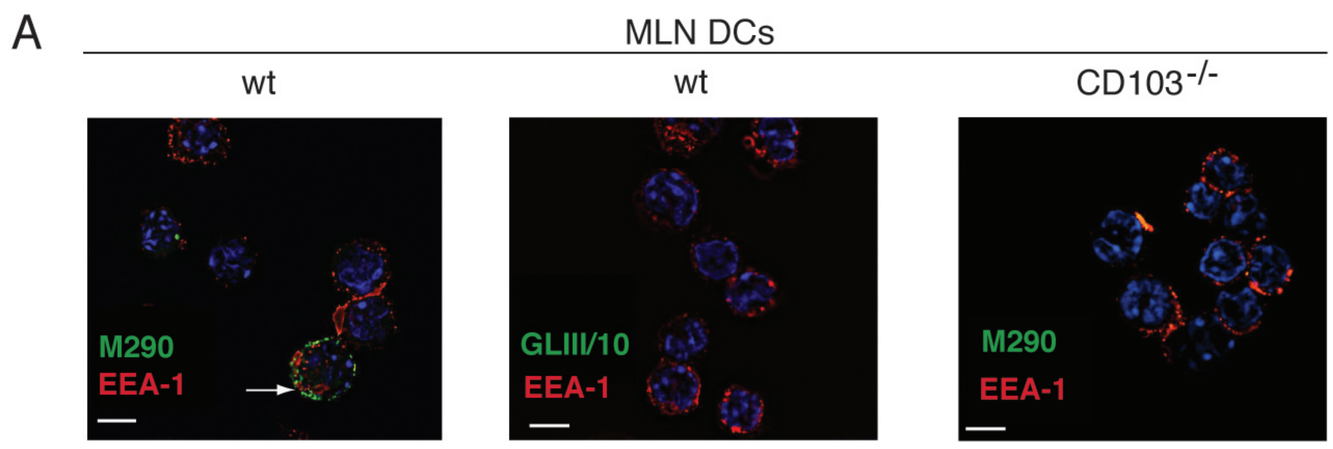

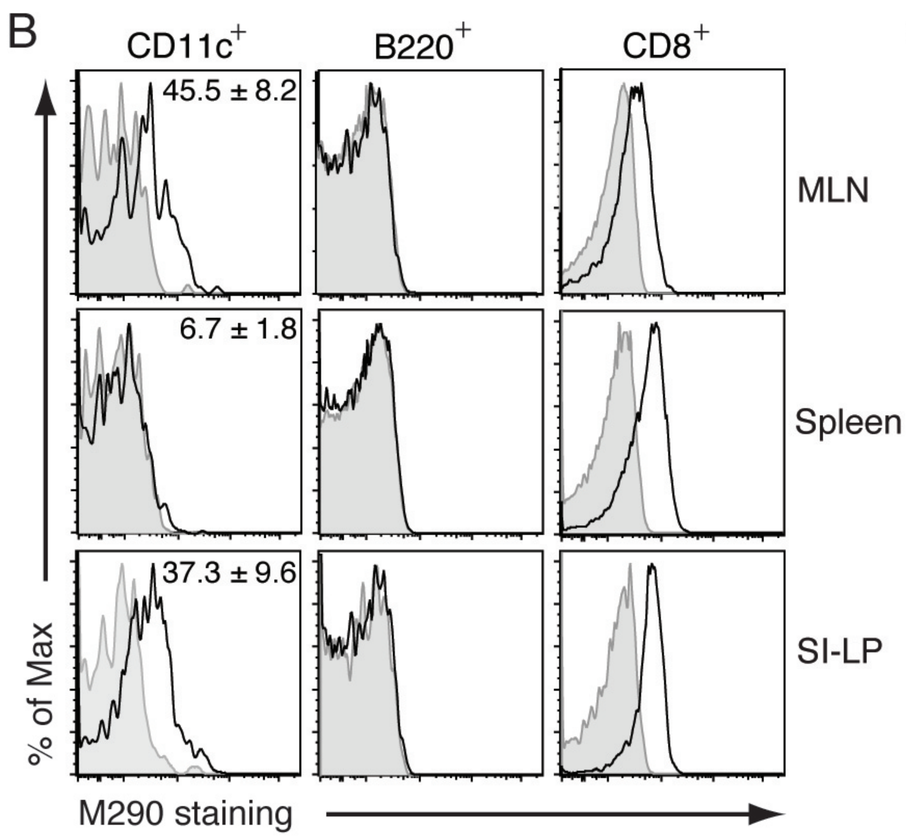

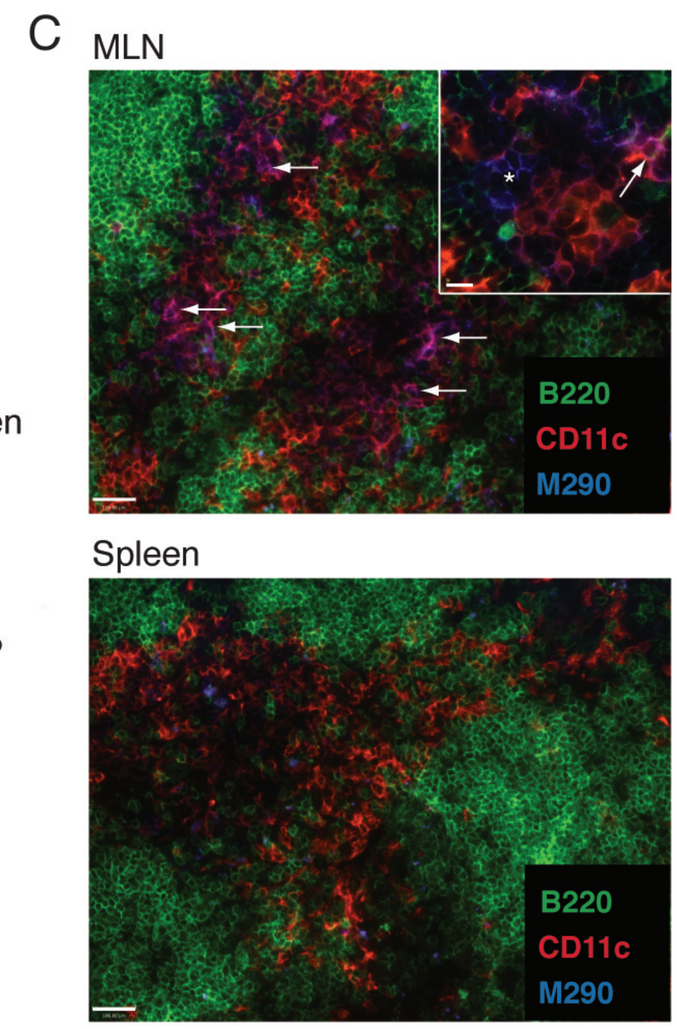

Supplementary Figure 2

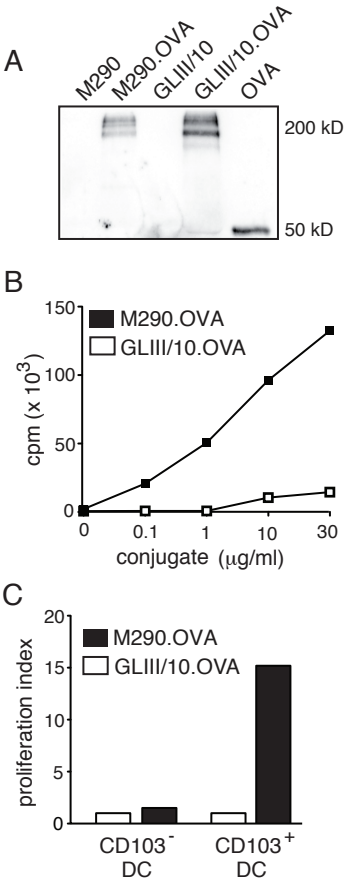

Supplementary Figure 3

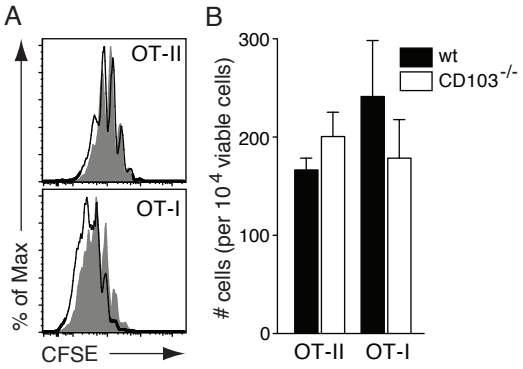

Supplementary Figure 4

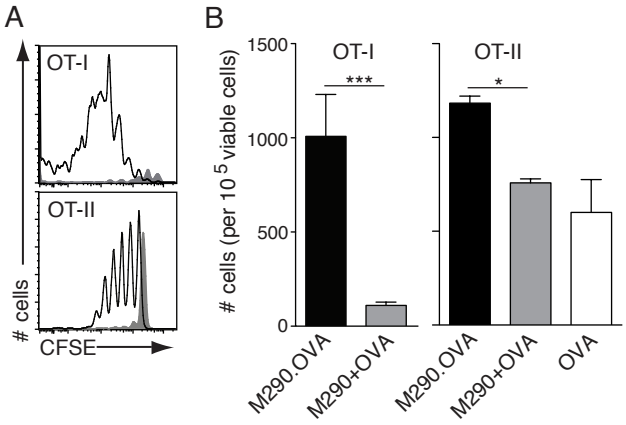

Supplementary Figure 5

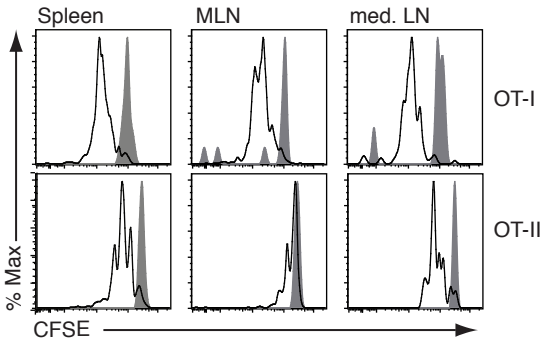

Supplementary Figure 6